Biosensors and Bioelectronics 99 (2018) 332–337

Contents lists available at ScienceDirect

Biosensors and Bioelectronics

journal homepage: www.elsevier.com/locate/bios

Profuse color-evolution-based fluorescent test paper sensor for rapid and visual monitoring of endogenous Cu^{2+} in human urine

Yueqing Cai, Junhui You, Zhengyi You, Fang Dong, Shuhu Du*, Liying Zhang*

School of Pharmacy, Nanjing Medical University, Nanjing, Jiangsu 211166, China

ARTICLE INFO

Keywords:
Fluorescent test paper
Sensor
Tricolor probe
Visual detection
Cu^{2+}

ABSTRACT

The fluorescent paper for colorimetric detection of metal ions has been widely fabricated using various sensing probes, but it still remains an elusive task to design a test paper with multicolor variation with target dosages for accurate determination. Herein, we report a profuse color-evolution-based fluorescent test paper sensor for rapid and visual monitoring of Cu^{2+} in human urine by printing tricolor probe onto filter paper. The tricolor probe consists of blue-emission carbon dots (bCDs), green-emission quantum dots (gQDs) and red-emission quantum dots (rQDs), which is based on the principle that the fluorescence of gQDs and rQDs are simultaneously quenched by Cu^{2+}, whereas the bCDs as the photostable internal standard is insensitive to Cu^{2+}. Upon the addition of different amounts of Cu^{2+}, the ratiometric fluorescence intensity of the tricolor probe continuously varied, leading to color changes from shallow pink to blue with a detection limit of 1.3 nM. When the tricolor probe solution was printed onto a sheet of filter paper, as-obtained test paper displayed a more profuse color evolution from shallow pink to light salmon to dark orange to olive drab to dark olive green to slate blue to royal blue and to final dark blue with the increase of Cu^{2+} concentration compared with dual-color probe-based test paper, and dosage scale as low as 6.0 nM was clearly discriminated. The sensing test paper is simple, rapid and inexpensive, and serves as a visual platform for ultrasensitive monitoring of endogenous Cu^{2+} in human urine.

1. Introduction

Recently, the quantification of metal ions is extensively performed by using conventional techniques, including atomic absorption spectroscopy (NG and Garner, 1993), mass spectrometry (Richardson, 2001), inductively coupled plasma-mass spectrometry (ICP-MS) (Bings et al., 2006), and so on. However, these techniques usually require ponderous instruments, the sophisticated sampling and professional operation by well-trained personnel, making it difficult to on-site monitor metal ions in environments and biological fluids. Therefore, there is an urgent demand for developing a simple, economical and portable method for *in vitro* and *in vivo* metal ions' assay, motivating considerable researchers to construct new miniature chemical sensors.

Semiconductor, such as quantum dots (QDs) or carbon dots (CDs), is a promising optical label for chemo/biosensing applications since it offers distinct advantages. These include (1) good optical properties, (2) good photochemical stability, (3) long fluorescence lifetime, and (4) good water solubility (Wang and Guo, 2009). Thus, it is a suitable candidate for fluorescent probe, which can be linked a recognition element to generate fluorescent "turn on", "turn off" or "ratiometric" response. Unfortunately, it still relies on fluorescent instrument, for example, fluorescent spectrometer or confocal microscope. To solve this problem, fluorescent test paper has been developed because it possesses an excellent and unparalleled merit, that is, its visualization capability for the detection of target analyte by the naked eye with the aid of a portable ultraviolet (UV) lamp. Generally, the fluorescent test paper is prepared by printing various fluorescent probes onto filter paper or microporous membrane. To date, fluorescent test paper utilizing a fluorescent single-color probe has been reported in many previous literatures, such as graphene oxide paper for the detection of peptide, protein, and DNA (Mei and Zhang, 2012), QDs paper for the assay of catechol and glucose (Yuan et al., 2012) and CDs paper for the analysis of mercuric ions (Yuan et al., 2014). But they can only exhibit the variation of fluorescence brightness by either "turn on" or "turn off" mode with analytes, which greatly limits their quantitative capability. More recently, test paper based on dual-emission fluorescent probe has been fabricated for the assay of trinitrotoluene by QDs@SiO_2-QDs paper (Zhang et al., 2011), the detection of sulfur dioxide by ratiometric QDs@SiO_2-QDs paper (Yan et al., 2015), the monitoring of pesticides by coumarin-3-carboxylic acid-QDs@SiO_2 paper (Li et al., 2015), the quantification of glucose by

* Corresponding authors.
E-mail addresses: shuhudu@njmu.edu.cn (S. Du), zly@njmu.edu.cn (L. Zhang).

http://dx.doi.org/10.1016/j.bios.2017.07.072
Received 23 May 2017; Received in revised form 17 July 2017; Accepted 29 July 2017
Available online 31 July 2017
0956-5663/

QDs@SiO_2-CDs paper (Huang et al., 2016), and so on. It is a pity that not only the fabrication procedure of dual-emission probe is complicated, but also the color variation of dual-emission probe is not profuse. So, multicolor-variation-based fluorescent test paper remains immature.

In this work, we present a fluorescent colorimetric method for dosage-sensitive and visual detection of Cu^{2+} by use of the tricolor probe system, which is fabricated by a simple blend of one blue CDs (bCDs) and two 3-mercaptopropionic acid (MPA)-functionalized QDs green QDs (gQDs) and red QDs (rQDs). With the increase of Cu^{2+} amount, photoluminescence (PL) intensity of gQDs and rQDs was gradually quenched, while the PL intensity of bCDs kept constant, accompanying continuous fluorescence color changes. Based on this, we develop a handy test strip by the assembly of the tricolor probe onto the filter paper for rapid monitoring of urinary copper, which is a promising auxiliary index for clinical diagnosis of Menkes (deficiency of copper) and Wilson's diseases (WD) (hyperaccumulation of copper) (Kaler, 2011; Burknead et al., 2011; Merle et al., 2007; Huster et al., 2006). The detail data are displayed below.

2. Experimental section

2.1. Reagents and instruments

3-Mercaptopropionic acid (MPA) was obtained from Sigma-Aldrich. Te powder, $NaBH_4$, $CdCl_2$•$2.5H_2O$, sulfuric acid (98%), NaOH, ethanol (95%), citric acid and ethylenediamine were purchased from Sinopharm Chemical Reagent Co., Ltd. (Shanghai, China). Rhodamine and KI were bought from Aladdin. HEPES (pH 7.4) was purchased from Sigma-Aldrich. All chemicals used were analytical grade. Ultrapure water (18.2 MΩ cm) was prepared by a Millipore water purification system.

UV–vis absorption and fluorescence spectra were recorded by Shimadzu UV-2450 (Japan) spectrophotometer and Hitachi F-4600 (Japan) fluorescence instrument, respectively. A JEOL JEM-2100 transmission electron microscope (TEM) instrument (Japan) was used to observe the morphology of nanoparticles. The hydrodynamic sizes of nanoparticles were determined using a Malvern Zetasizer Nano-ZS90 (UK) particle size analyzer. FT-IR spectra were recorded on a TENSOR 27 spectrometer (Bruker, Germany) with a resolution of 2 cm^{-1} and a spectral range of 4000–400 cm^{-1}. X-ray photoelectron spectroscopy (XPS) spectra were collected on a PHI Quantera II spectrometer (Japan). To assess accuracy of the method, urine samples were also analyzed on an ICP-MS (iCAP Q, Thermo Fisher, America). Fluorescent photos were taken under an AGL-9406 UV lamp (China) with a Canon 600D digital camera (Japan).

2.2. Synthesis of CDs

Blue-emission CDs were prepared by the previously reported method (Huang et al., 2016). Briefly, 1.05 g of citric acid and 0.34 mL of ethylenediamine were first dissolved in 20 mL ultrapure water. Then the solution was transferred to a polytetrafluoroethylene autoclave (30 mL) and heated at 200 °C for 5 h. After gradually cooled to room temperature, the resultant bCDs were purified by dialysis for 24 h.

2.3. Synthesis of CdTe QDs

QDs were prepared by the method of previous literature (Zhou et al., 2016). Typically, 0.06 g Te powder and 0.1 g $NaBH_4$ were first mixed in 2 mL of ultrapure water under nitrogen atmosphere in an ice bath, then stirred for 6 h to get the NaHTe solution. Meanwhile, 0.228 g of $CdCl_2$•$2.5H_2O$ and 210 μL of MPA were dissolved in 100 mL of ultrapure water and adjusted pH to 9 with 1.0 M NaOH, and the mixing solution was deoxygenated by bubbling nitrogen for 30 min. Subsequently, 5 mL of H_2SO_4 (0.5 M) was injected into the as-obtained NaHTe solution and the timely produced H_2Te gas was inlet into the above mixing solution of $CdCl_2$ and MPA until the solution color transformed from colorless to orange. After refluxing for 1 h, gQDs with an emission at 510 nm were synthesized. The synthesis of rQDs with an emission at 600 nm was performed in a similar way, but varying the time of reflux (24 h). The prepared QDs were rinsed with acetone and dispersed in 100 mL of ultrapure water for further use.

2.4. Preparation of fluorescent test papers

The tricolor probe-based fluorescent test papers were prepared as described in our previous work (Zhou et al., 2016). Briefly, a common cartridge of a commercial inkjet printer was washed with ultrapure water until the ink powder was cleared away completely, followed by drying in an oven at 50 °C for 6 h. The tricolor probe solution as ink was into the vacant cartridge. A rectangle pattern of 7 × 3 cm^2 was printed on a piece of filter paper by the printer connected to a computer, and the printing was repeated for 30 times. After air-drying for 15 min, the pattern was cut into 3 × 1 cm^2 pieces for the visual detection of Cu^{2+}. For comparison, the dual-color probe-based fluorescent test papers were also fabricated using the same method, but replacing the tricolor probe with dual-color probe.

2.5. Colorimetric detection of Cu^{2+} in human urine

With the patients' informed-consent, 24-h urine samples of four patients with WD were obtained from the First Affiliated Hospital of Anhui University of Chinese Medicine. Moreover, normal urine samples were also collected from three healthy volunteers in a period of 24 h. Prior to the assay, all urine samples were filtered through 0.45 μm Supor filters to remove any particulate suspension, then stored in refrigerator at 4 °C until further analysis.

Fluorescent measurement of Cu^{2+}: Different amounts of Cu^{2+} were added into the tricolor probe solution with HEPES buffer (pH 7.4) and thoroughly mixed for 30 s, and the fluorescent spectra were recorded with a spectrometer.

Detection of Cu^{2+} on test paper: Each urine sample (500 μL) was dropped onto the as-obtained test paper, and after that the corresponding color of test paper was observed under a 365 nm UV lamp.

3. Results and discussion

3.1. Characterization of QDs and CDs

Fig. 1 shows the fluorescence spectra of bCDs, gQDs, rQDs and tricolor probe. The bCDs, gQDs and rQDs display a maximal emission

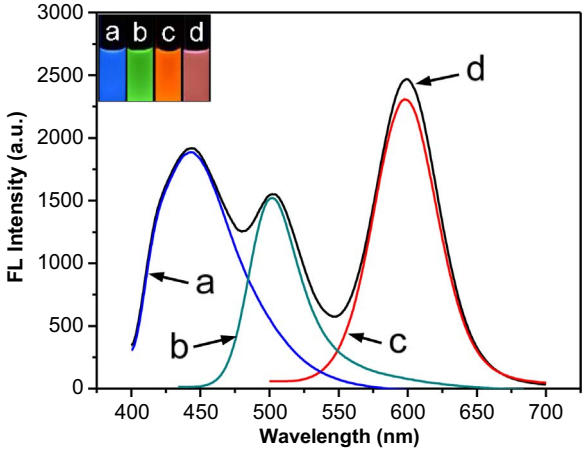

Fig. 1. Fluorescence emission spectra (λ_{ex} = 360 nm) of (a) bCDs, (b) gQDs, (c) rQDs and (d) the tricolor probe (the inset photos were taken under 365 nm UV lamp).

wavelength at 440 nm, 510 nm and 600 nm, emitting bright blue, green and red fluorescence under a 365 nm UV lamp (Fig. 1, inset images a, b and c), respectively. The tricolor probe can exhibit ternary-emission bands at 440, 510 and 600 nm under a single wavelength (at 360 nm) excitation and displays a shallow pink fluorescence, which is different from that of bCDs, gQDs and rQDs (Fig. 1, inset image d). Moreover, the architectures of CDs and QDs were also studied in detail. The used bCDs, gQDs and rQDs were ~ 3, ~ 3 and ~ 7 nm in size by the observation of TEM (Fig. S1A, C and E), respectively. Meanwhile, dynamic light scattering gave the hydrate particle sizes of ~ 6, ~ 5 and ~ 15 nm for bCDs, gQDs and rQDs, respectively (Fig. S1B, D and F), which were much larger than the sizes themselves due to the formation of hydration layer, revealing that bCDs, gQDs and rQDs had the excellent hydrophilicity. To further confirm the surface status information on CDs and QDs, FT-IR measurements were carried out. As showed in Fig. S2 (curve a and b), the appearance of two bands at ~ 1570 cm^{-1} and 1402 cm^{-1} as the characteristic -COOH vibration of MPA (Abd El-sadek et al., 2010) proved that MPA covalently bound to the surface of QDs. The bCDs displayed many characteristic peaks at 3415 cm^{-1} (the stretching vibration of C-OH), 3000 cm^{-1} (the stretching vibration of C-H), 1570 cm^{-1} (bending vibrations of N-H) and 1709 cm^{-1} (the vibrational absorption band of C=O) (Fig. S2, curve c). These spectra data suggest that numerous nitrogen-containing and oxygen-containing groups exist on the surface of CDs or QDs, which are responsible for high aqueous solubility.

3.2. Red-green-blue (RGB)-based colorimetric principle

It is known that the wide color-changing test papers are usually prepared by use of colorful fluorescent probes. Scheme 1 illustrates three representative states on the ranges of color variation when two or three probes among red-green-blue colors are simultaneously employed together. As indicated with the arrow in Scheme 1A, the equal proportional mixture of red and blue probes produces a purple, leading to that the maximal change ranges from purple to blue or purple to red, which greatly compresses the range of color variation. To avoid this situation, the proportion of red and blue probes may be adjusted. When the proportion of blue to red is 1:3, the dual-color probe displays a plum red, so the color-varying range can be enlarged (from plum red to blue) (Scheme 1B). However, its color variation is still limited. Herein, we present a distinctive tricolor probe by integrating three probes (bCDs, gQDs and rQDs) with different ratios in one system, which not only ensures the widest color-varying range but also exhibits more profuse color variation (Scheme 1C).

3.3. Fluorescent quenching mechanism of the tricolor probe by Cu^{2+}

Fig. 2 shows the fluorescent dual-quenching mechanism for visual detection of Cu^{2+}. In the ternary-emission probe system, the

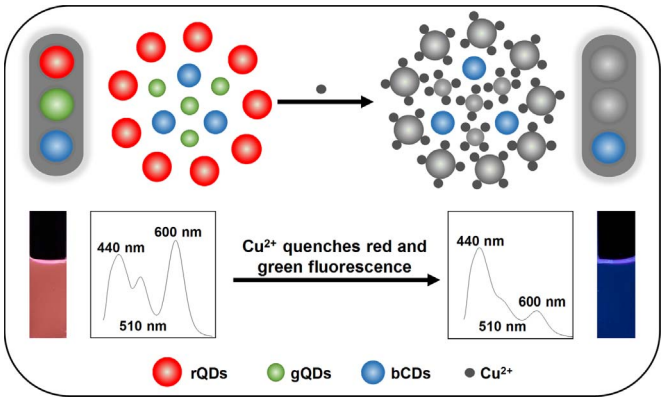

Fig. 2. Schematic illustration of the visual detection principle for Cu^{2+} using the tricolor probe.

bCDs have high stability (Fig. S3) and no obvious fluorescent response to Cu^{2+} (Fig. S4), providing a reliable reference signal for colorimetric detection of Cu^{2+}. But the gQDs and rQDs, acting as signaling units, can be simultaneously quenched by Cu^{2+}. To better elucidate the role of Cu^{2+} in quenching the QDs PL, XPS measurements were performed in an effort to investigate the mechanism of the selective Cu^{2+} response of CdTe QDs. Fig. S5 shows high-resolution spectra of the C(1s), S(2p), Cd(3d), Te(3d) and Cu(2p) regions after treating the CdTe QDs with ultrapure water (upper row) and 1 mM Cu^{2+} (bottom row). After treating the CdTe QDs with Cu^{2+}, high-resolution photoelectron spectra of the Cu(2p) displayed two peaks centering at 931.2 ± 0.1 and 951.2 ± 0.1 eV, which corresponded to the Cu($2p_{3/2}$) and Cu($2p_{1/2}$), respectively. The peaks were characteristic of Cu^{+} rather than Cu^{2+} (Goh et al., 2006; Nakai et al., 1978), suggesting the presence of only Cu^{+} on the surface of QDs. This was consistent with the thermodynamically allowed reduction of Cu^{2+} to Cu^{+} by Te^{2-} of QDs, as previously shown by Isarov and Chrysochoos (1997). Meanwhile, we also examined the CdTe QDs by XPS after treatment with Ca^{2+}, K^{+}, Mg^{2+} or Zn^{2+}, as the potential ions in human urine, and no visible peak was detected (Fig. S6), demonstrating the excellent selectivity of the tricolor probe to Cu^{2+}. On the other hand, as shown in the UV–vis absorption spectra (Fig. S7), the bCDs, gQDs and rQDs had almost no absorption in the visible region, suggesting that there was no energy transfer among the bCDs, gQDs and rQDs. Moreover, the emission spectra of QDs and the UV–vis absorption spectrum of Cu^{2+} also had not overlap with each other (Fig. S8), indicating that the resonance energy transfer would not be the prominent pathway of quenching mechanism. Thus, the quenching pathway of QDs by Cu^{2+} is the reduction of surface adsorbed Cu^{2+} to form nonradiative surface channels (Wu et al., 2014).

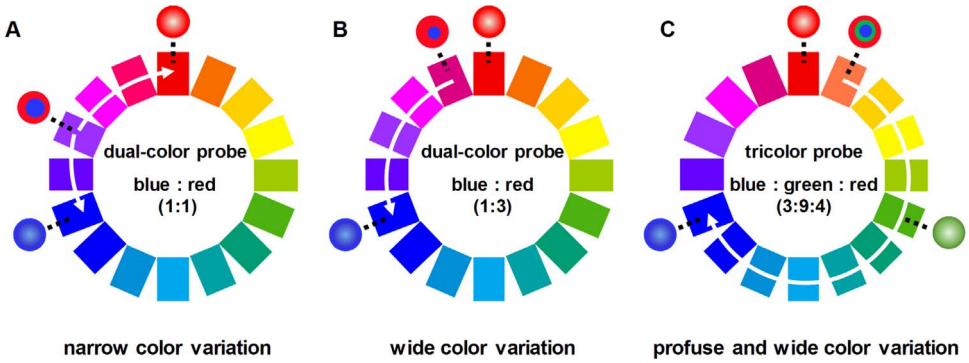

Scheme 1. RGB-based colorimetric assay on the range of color variation while the different color probes are coexisted in a sensing system: (A) 1:1 dual-color probe; (B) 1:3 dual-color probe and (C) 3:9:4 tricolor probe. The arrows indicate the ranges of color variations.

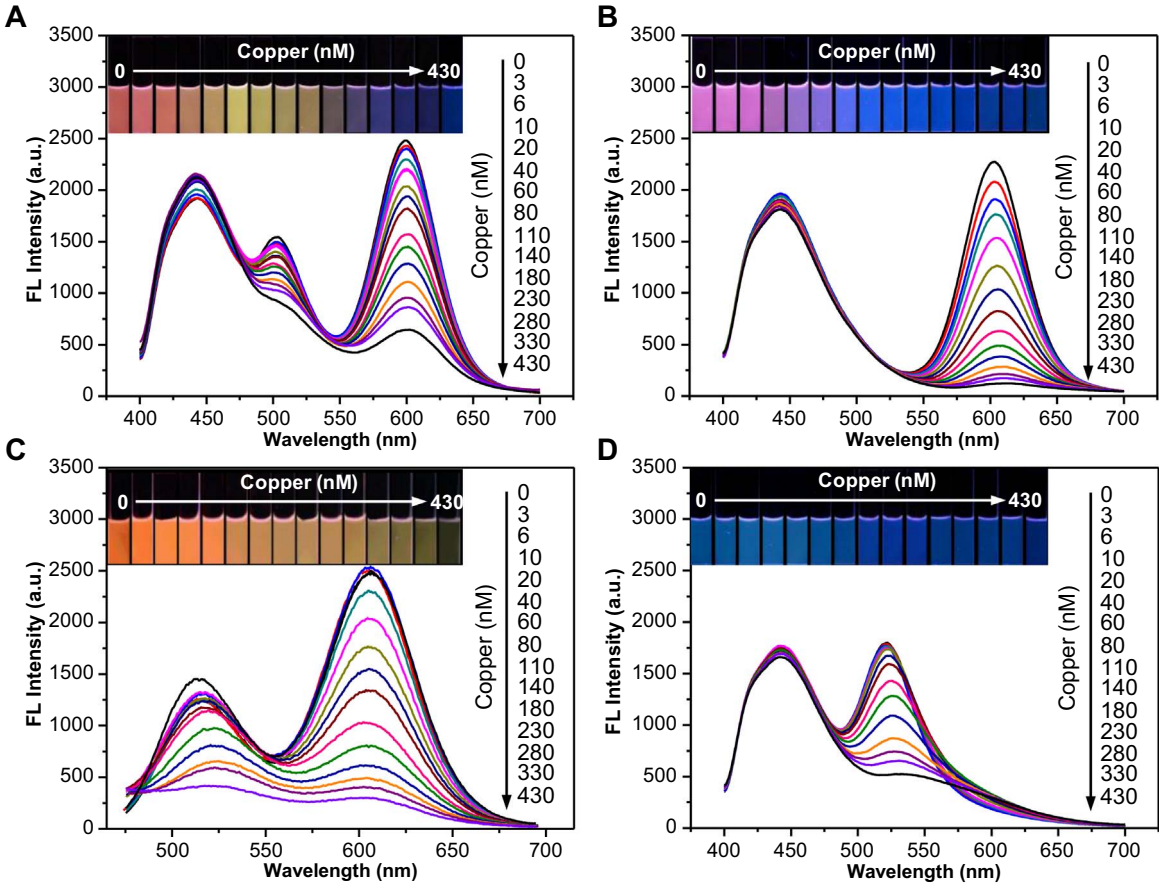

Fig. 3. Fluorescent spectra of the mixing probes at different ratios with the addition of Cu^{2+}. The ratios of (A) bCDs to gQDs to rQDs, (B) bCDs to rQDs, (C) gQDs to rQDs and (D) bCDs to gQDs were 3:9:4, 3:4, 9:4 and 3:9, respectively. The insets show the corresponding fluorescent photos taken under 365 nm UV lamp.

3.4. Sensitive response and selectivity of the fluorescent tricolor probe to Cu^{2+}

Prior to the sensitivity study, the response time of the tricolor probe to Cu^{2+} was first investigated. With addition of 100 nM Cu^{2+}, the ratios of fluorescence intensities, I_{440}/I_{510} and I_{440}/I_{600}, rapidly increased and then reached constant when the response time was up to 30 s, indicating that it was a very quick process for the fluorescence quenching of the tricolor probe by Cu^{2+} (Fig. S9). So, the response time 30 s is used as the optimized detection time throughout the following works. Fig. 3 shows the evolution of fluorescent spectra of the tricolor probe and dual-color probe with the titration of Cu^{2+}. Upon the addition of Cu^{2+}, the fluorescence intensities (at 510 nm and 600 nm) of gQDs and rQDs were gradually quenched, whereas the fluorescence intensity at 440 nm of bCDs still stayed highly steady (Fig. 3A). Due to the change of ratio of fluorescence intensities at three emission wavelengths, a profuse and wide color variation (from shallow pink to light salmon to dark orange to olive drab to dark olive green to slate blue to royal blue and to final dark blue) was observed in the inset of Fig. 3A. Obviously, even a slight decrease of the emission intensities at 510 nm and 600 nm resulted in distinguished color changes from the initial background, so the visualization assay of Cu^{2+} by the naked eye under a portable UV lamp is feasible.

Furthermore, the volume ratio of blue to green to red for fabricating the tricolor probe was also optimized to improve the visual effect. As shown in Fig. S10, the best visual effect of color variation was obtained at the 3:9:4 ratio of blue to green to red in volume. Under the optimal condition, the ratio of fluorescence intensities, $I_{440}/(I_{510}+I_{600})$, displayed a dosage-dependence with good linearity against Cu^{2+} concentrations in the range of 3–430 nM with correlation coefficient R^2 = 0.9943 (Fig. S11) and the detection limit reached as low as 1.3 nM based on the definition of 3 times the deviation of the blank signal (3σ, where σ is the standard deviation for ten blank measurements). The advantage of the tricolor probe (dual fluorescence quenching) for visual detection of Cu^{2+} was further validated by the comparison with the dual-color probe (single fluorescence quenching). As shown in the inset of Fig. 3B and C, the fluorescent color variation of the dual-color probe (either bCDs and rQDs or gQDs and rQDs) upon addition of Cu^{2+} was inferior to that of the tricolor probe. However, the color change of another dual-color probe (bCDs and gQDs) with addition of Cu^{2+} was little observed (the inset of Fig. 3D). These comparisons clearly exhibit that the tricolor probe possesses better naked eye recognition than dual-color probe for visual detection of Cu^{2+}.

In order to evaluate the selectivity of the tricolor probe to Cu^{2+}, the change of fluorescence intensity ratio, $I_{440}/(I_{510}+I_{600})$, was observed at the same conditions with various other metal ions, including Ba^{2+}, K^{+}, Mn^{2+}, Co^{2+}, Pb^{2+}, Fe^{3+}, Ni^{2+}, Al^{3+}, As^{5+}, Cd^{2+}, Na^{+}, Zn^{2+}, Mg^{2+}, Fe^{2+}, Ca^{2+} and Hg^{2+}. By comparison, the fluorescence intensity ratio $I_{440}/(I_{510}+I_{600})$ and color were unchanged in the presence of other metal ions (except Hg^{2+}), indicating that the superior selectivity of the tricolor probe to Cu^{2+} (Fig. 4). Although Hg^{2+} ion disturbed the detection of Cu^{2+}, the interference was easily suppressed by a simple sample pretreatment with KI, NaCl and Rhodamine B (Fig. S12), which was based on the formation of an ion-associate of HgI_4^{2-} and RhB (Liu et al., 1983). Moreover, the anti-interference test of Cu^{2+} detection was also performed in the coexistence of the other metal ions. With the addition of Cu^{2+} (0.3 μM) containing other metal ions (3.0 μM) into the tricolor probe solution, the fluorescence intensity ratio $I_{440}/(I_{510}+I_{600})$ was unaffected by 10-fold excesses of the interfering metal ions. These results reveal that the tricolor probe shows selectivity and specificity for Cu^{2+} over the other metal ions.

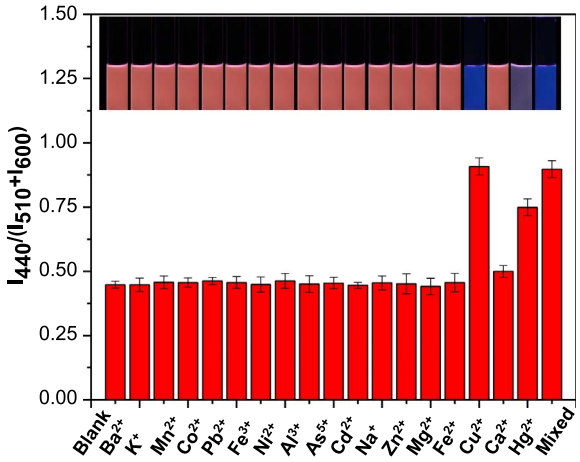

Fig. 4. The selectivity of fluorescent tricolor probe to different metal ions. The concentration of Cu^{2+} used is 0.3 μM, and those of other metal ions are all 3 μM. The insets show the corresponding fluorescent photos under 365 nm UV lamp.

Due to the sensitivity and selectivity of the tricolor probe to Cu^{2+}, we further investigated capability of it for detecting endogenous Cu^{2+} in healthy people and WD patient urine samples. Prior to the assay, the patient urine samples were diluted 100 times with ultrapure water so that the level of Cu^{2+} was within the linear ranges. The analytical data were summarized in Table S1. As shown in Table S1, we found that the obtained results by ICP-MS technique were slightly higher than those by the proposed method. It is because that the ICP-MS data is responsive to the total concentration of copper, rather than Cu^{2+} concentration. When the known amount of Cu^{2+} (100.0 nM) was added in healthy human urine samples, the recovery of Cu^{2+} ranged from 99.3% to 101.0% (Table S1). These confirm that the tricolor probe has high accuracy and reliability to satisfy the requirements of practical application.

3.5. Fluorescent test paper-based sensor for rapid monitoring of Cu^{2+} in human urine

To prepare the test paper, the mixture of bCDs, gQDs and rQDs (3:4:9 in volume) as ink was jet-printed onto a sheet of filter paper (which was nonfluorescent under 365 nm UV lamp to avoid the interference to visual colorimetry) by the control of a computer and air drying at room temperature for 15 min prior to assay. The preparation procedure made the probe evenly stick to the substrate of paper fiber, avoiding disassociations from paper after contacting target solution (Fig. S13). The test paper stored at 4 °C fridge was stable in 60 days (Fig. S14). After the aqueous solution of Cu^{2+} was evenly added onto the test paper, the surprising color variation with the dosages of Cu^{2+} could be observed under UV lamp. As indicated in Fig. S15A, each dosage from 0 to 430 nM matched an eye-recognized color from shallow pink to light salmon to dark orange to olive drab to dark olive green to slate blue to royal blue and to final dark blue, which was in a good agreement with the result above (Fig. 3A). Importantly, the pink of the test paper at even 6 nM Cu^{2+} was lighter than that at 0 nM but different from that (dark orange) at 20 nM, indicating the distinguished dosage scale as low as 6 nM. Meanwhile, the color variation of fluorescent test paper made by the dual-color probe (either bCDs and rQDs or gQDs and rQDs) was apparently very limited (Fig. S15B and C). So, we can imagine that the performance of test paper made of bCDs and gQDs is identical to the case of pure bCDs and gQDs solution (data not shown).

A practical on-spot analyzer depends on the rapid and visual recognition and determination of target analyte. In this work, we further demonstrated that the fluorescent test paper could be employed for rapid and visual monitoring of Cu^{2+} in human urine. Generally, the upper limit of copper in normal human urine is 0.6 μmol/24 h (Ala et al., 2007), and the reference limit of copper in WD patient urine is greater than 1.6 μmol/24 h (Chappuis et al., 2007). As shown in Fig. 5, the fluorescent colors at 30.4, 149.1, 21.3 and 39.2 nM Cu^{2+} (equal to 5.3, 9.4, 8.7 and 8.2 μmol/24 h) in four WD patient urine samples were accordant with the corresponding colors in Fig. S15A, respectively, suggesting a discernible dosage capability by the naked eye. Meanwhile, for the three normal human urine samples, similar results were also obtained, but each urinary copper level was far lower than that of WD patient (Fig. S16 and Table S1). Thus, the test paper sensor can provide a clear and fast judgment whether the human urinary copper is at a normal or abnormal level for the clinical diagnosis of WD.

3.6. Comparison of the proposed method and other works

The above results have validated the feasibility of the developed method for the determination of Cu^{2+}. Compared to other methods, the detection limit of as-developed method is lower than that of flame atomic absorption spectrometry (FAAS) (Lima et al., 2012), anodic stripping voltammetry (ASV) (Shao et al., 2013), electrochemical sensor (Jasmin et al., 2016), colorimetry (Dhar et al., 2015; Tang et al., 2017), immunoassay (Ouyang et al., 2016), surface-enhanced Raman spectroscopy (SERS) (Li et al., 2017) and spectrofluorometry (Dong et al., 2012). Although The ICP-MS (Dai et al., 2012) has higher sensitivity than the proposed method, it requires large-scale instrument and highly trained operator, restricting the practical on-site detection. Moreover, two spectrofluorometric methods (Yao et al., 2013; Jin and Han, 2014) also provide a relatively lower detection limit, but they can't realize colorimetry-based visual quantification.

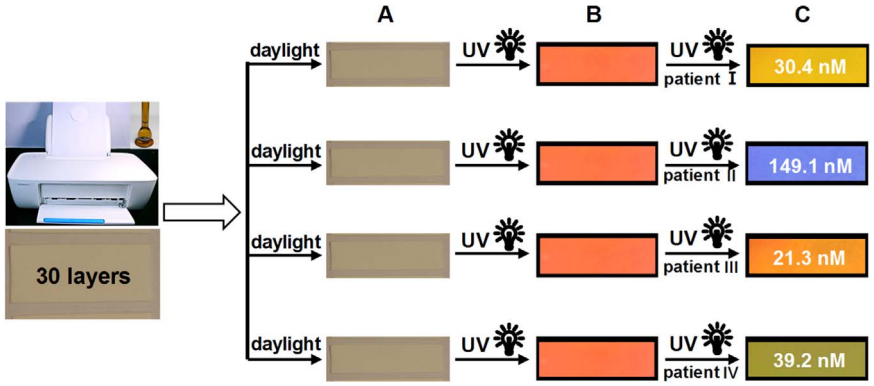

Fig. 5. The preparation procedure of test papers and visual detection of Cu^{2+} in patient urine samples. Each sample was diluted 100-fold before the addition onto test papers. The photos of test papers were taken (A) under daylight, (B) under UV lamp and (C) after the addition of real urine samples under UV lamp.

Meanwhile, even though another spectrofluorometry (in which rQDs-bCDs serves as the dual-color probe) (Wang et al., 2016) has essentially realized the visual detection of Cu^{2+}, our proposed test paper has more profuse color variation with the increase of Cu^{2+}(Table S2). In a word, the method proposed herein is simple and inexpensive, each test is achieved within ~ 1 min and is sufficient to monitor Cu^{2+} at the upper limit in normal human urine.

4. Conclusions

We have fabricated a profuse and wide color varying fluorescent test paper sensor for the dosage-dependent and visual analysis as classical pH test paper. It has been demonstrated that the tricolor probe possesses superior selectivity and ultra-high sensitivity to Cu^{2+} and as-fabricated test paper displays a continuous color change with the increase of Cu^{2+} amount. Moreover, a discerning dosage response to Cu^{2+} in human urine was observed by the naked eye. The advantages of this work mainly include the following three points: (1) it is very simple to construct the tricolor probe, avoiding the complex prepared procedures by covalent bonding between CDs and QDs; (2) the handy test paper is convenient to operate for a nonprofessional operator, compared to other analytical technologies; and (3) importantly, the high-quality test paper provides a profuse and wide color variation for visual detection of Cu^{2+} compared with the test paper made of the dual-color probe reported in previous literatures. In brief, the fluorescent test paper sensor provides an efficient and available tool for metal detection directly from biological samples with minimal pretreatment (only filtration). We believe that this test paper increases vast possibilities for visual on-site monitoring other target analytes in various fields, especially for healthcare and public safety.

Acknowledgment

This work is supported by the National Natural Science Foundation of China (21275075, 61605084).

Appendix A. Supplementary material

Supplementary data associated with this article can be found in the online version at doi:10.1016/j.bios.2017.07.072.

References

Abd El-sadek, M.S., Kumar, J.R., Moorthy Babu, S., 2010. Curr. Appl. Phys. 10, 317–322.
Ala, A., Walker, A.P., Ashkan, K., Dooley, J., Schilsky, M.L., 2007. Lancet 369, 397–408.
Bings, N.H., Bogaerts, A., Broekaert, J.A.C., 2006. Anal. Chem. 78, 3917–3946.
Burknead, J.L., Gray, L.W., Lutsdenko, S., 2011. BioMetals 24, 455–466.
Chappuis, P., Callebert, J., Quignon, V., Woimant, F., Laplanche, J.L., 2007. J. Trace Elem. Med. Biol. 21, 37–42.
Dai, B.Y., Cao, M.R., Fang, G.Z., Liu, B., Dong, X., Pan, M.F., Wang, S., 2012. J. Hazard. Mater. 219, 103–110.
Dhar, P.C., Pal, A., Mohanty, P., Bag, B., 2015. Sens. Actuators B 219, 308–314.
Dong, Y.Q., Wang, R.X., Li, G.L., Chen, C.Q., Chi, Y.W., Chen, G.N., 2012. Anal. Chem. 84, 6220–6224.
Goh, S.W., Buckley, A.N., Lamb, R.N., 2006. Miner. Eng. 19, 204–208.
Huang, X.Y., Zhou, Y.J., Liu, C., Zhang, R.L., Zhang, L.Y., Du, S.H., Liu, B.H., Han, M.Y., Zhang, Z.P., 2016. Biosens. Bioelectron. 86, 530–535.
Huster, D., Finegold, M.J., Morgan, C.T., Burkhead, J.L., Nixon, R., Vanderwerf, S.M., Gilliam, C.T., Lutsenko, S., 2006. Am. J. Pathol. 168, 423–434.
Isarov, A.V., Chrysochoos, J., 1997. Langmuir 13, 3142–3149.
Jasmin, J.P., Ouhenia-Ouadahi, K., Miserque, F., Dumas, E., Cannizzo, C., Chaussé, A., 2016. Electrochim. Acta 200, 115–122.
Jin, L.H., Han, C.S., 2014. Anal. Chem. 85, 7209–7213.
Kaler, S.G., 2011. Nat. Rev. Neurol. 7, 15–29.
Li, C.N., Ouyang, H.X., Tang, X.P., Wen, G.Q., Liang, A.H., Jiang, Z.L., 2017. Biosens. Bioelectron. 87, 888–893.
Li, H.H., Zhu, H.J., Sun, M.T., Yan, Y.H., Zhang, K., Huang, D.J., Wang, S.H., 2015. Langmuir 31, 8667–8671.
Lima, G.F., Ohara, M.O., Clausen, D.N., Nascimento, D.R., Ribeiro, E.S., Segatelli, M.G., Bezerra, M.A., Tarley, C.R.T., 2012. Microchim. Acta 178, 61–70.
Liu, S.P., Liu, Y., Liu, Z.F., 1983. Mikrochim. Acta 3, 355–366.
Mei, Q.S., Zhang, Z.P., 2012. Angew. Chem. Int. Ed. 51, 5602–5606.
Merle, U., Schaefer, M., Ferenci, P., Stremmel, W., 2007. Gut 56, 115–120.
NG, K.C., Garner, T.J., 1993. Appl. Spectrosc. 47, 241–243.
Nakai, I., Sugitani, Y., Nagashima, K., Niwa, Y., 1978. J. Inorg. Nucl. Chem. 40, 789–791.
Ouyang, H., Shu, Q., Wang, W.W., Wang, Z.X., Yang, S.J., Wang, L., Fu, Z.F., 2016. Biosens. Bioelectron. 85, 157–163.
Richardson, S.D., 2001. Chem. Rev. 101, 211–254.
Shao, X.L., Gu, H., Wang, Z., Chai, X.L., Tian, Y., Shi, G.Y., 2013. Anal. Chem. 85, 418–425.
Tang, S.R., Wang, M.L., Li, Z.J., Tong, P., Chen, Q., Li, G.W., Chen, J.H., Zhang, L., 2017. Biosens. Bioelectron. 89, 866–870.
Wang, X., Guo, X.Q., 2009. Analyst 134, 1348–1354.
Wang, Y.H., Zhang, C., Chen, X.C., Yang, B., Yang, L., Jiang, C.L., Zhang, Z.P., 2016. Nanoscale 8, 5977–5984.
Wu, P., Zhao, T., Wang, S.L., Hou, X.D., 2014. Nanoscale 6, 43–64.
Yao, J.L., Zhang, K., Zhu, H.J., Ma, F., Sun, M.T., Yu, H., Sun, J., Wang, S.H., 2013. Anal. Chem. 85, 6461–6468.
Yan, X., Li, H.X., Zheng, W.S., Su, X.G., 2015. Anal. Chem. 87, 8904–8909.
Yuan, C., Liu, B.H., Liu, F., Han, M.Y., Zhang, Z.P., 2014. Anal. Chem. 86, 1123–1130.
Yuan, J.P., Gaponik, N., Eychmüller, A., 2012. Anal. Chem. 84, 5047–5052.
Zhang, K., Zhou, H.B., Mei, Q.S., Wang, S.H., Guan, G.J., Liu, R.Y., Zhang, J., Zhang, Z.P., 2011. J. Am. Chem. Soc. 133, 8424–8427.
Zhou, Y.J., Huang, X.Y., Liu, C., Zhang, R.L., Gu, X.L., Guan, G.J., Jiang, C.L., Zhang, L.Y., Du, S.H., Liu, B.H., Han, M.Y., Zhang, Z.P., 2016. Anal. Chem. 88, 6105–6109.